Journal Name

COMMUNICATION

Chiral recognition at self-assembled multivalent (SAMul) nanoscale interfaces – enantioselectivity in polyanion binding

Received 00th January 20xx,
Accepted 00th January 20xx

DOI: 10.1039/x0xx00000x

www.rsc.org/

Ching W. Chan,[a] Erik Laurini,[b] Paola Posocco,[b] Sabrina Pricl,[b] and David K. Smith*,[a]

Self-assembled multivalent (SAMul) ligands based on palmitic acid functionalised with cationic L/D-lysine bind polyanionic heparin or DNA with no chiral preference. Inserting a glycine spacer unit switches on chiral discrimination – a rare example of controlled chiral recognition at a SAMul nanoscale interface.

Molecular recognition at self-assembled surfaces is a key strategy used by biological systems to organise ligands over nanometre length scales, enabling adhesion to biomolecular targets.[1] There is increasing interest in synthetic supramolecular systems which bind nanoscale biological targets,[2] with multivalent binding being of particular use.[3] Self-assembly is a powerful strategy to organise such interactions.[4] We have been developing self-assembled multivalent (SAMul) systems to bind polyanions such as DNA[5] and heparin,[6] which have potential clinical relevance in gene therapy,[7] and blood coagulation control,[8] respectively. More broadly, it is worth noting that there are many polyanions in biological systems – including cell membranes, microfilaments and tubules. Biology can control these polyanions with precise selectivity – understanding and intervening in this remains a real challenge.[9] Self-assembled polycations are widely used to bind polyanions.[10] Selectivity at such binding interfaces is primarily considered to be based on charge density;[11] other factors are known to modulate selectivity, but the number of experimental examples is limited.[12] We have therefore been interested in exploring the subtleties of polyanion recognition. We recently studied ligand modification in SAMul systems and found different polyanions exhibited different ligand preferences.[13] We have also studied chiral systems, and found ligand chirality could enable enantioselective binding.[14] Chiral micelles are known to separate enantiomers in capillary electrophoresis, with the low-molecular-weight analyte partitioning into the micelle, close to the surfactant chiral centre,[15] but this is somewhat different to our report of chiral multivalent binding across the self-assembled surface.[14] However, the molecular structures in our previous report were relatively complex, and we therefore wanted to simplify our molecular design to probe the impact of simple structural modifications on chiral ligand display.

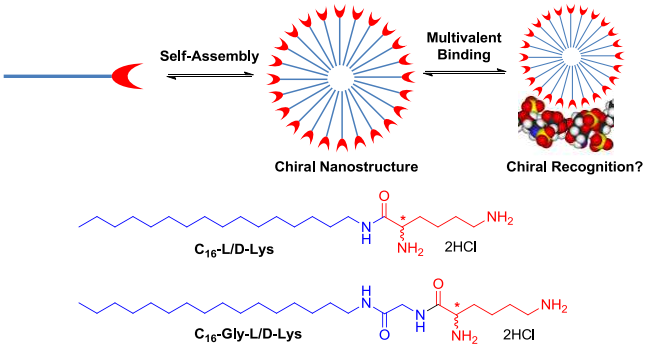

Figure 1. Compounds investigated in this paper. and schematic of self-assembled multivalent (SAMul) binding of polyanions.

In our new minimal design, Boc-protected L- or D-Lysine was coupled with 1-hexadecylamine using TBTU and Et_3N in DCM, with the desired compounds C_{16}-L-Lys and C_{16}-D-Lys being obtained after removal of the protecting groups using HCl gas in methanol. Similarly, the glycine-spaced compounds were synthesised using solution-phase TBTU-mediated peptide coupling and a Boc-protecting group strategy (see ESI). The syntheses worked in good yields, with circular dichroism (CD) spectroscopy being used to confirm enantiomeric relationships; each pair of compounds exhibited mirror-image spectra (Table 1 and ESI). The CD spectra of the compounds with and without a glycine spacer were different, reflecting the presence of the additional UV-chromophoric peptide bond.

We probed the critical aggregation concentrations (CACs) using a Nile Red assay in PBS buffer.[16] The CACs of C_{16}-L-Lys and C_{16}-D-Lys were 33 ± 3 μM and 29 ± 4 μM respectively, while those of C_{16}-Gly-L-Lys and C_{16}-Gly-D-Lys were 31 ± 3 μM and 28 ± 3 μM (Table 1). As such, all compounds had similar CACs, and as expected, the enantiomers behaved identically

[a] Department of Chemistry, University of York, Heslington, York, YO10 5DD, UK. Email: david.smith@york.ac.uk
[b] Simulation Engineering (MOSE) Laboratory, Department of Engineering and Architectures (DEA), University of Trieste, Trieste, 34127, Italy

Electronic Supplementary Information (ESI) available: full synthesis and characterisation data, assay methods, additional assay data and imaging. See DOI: 10.1039/x0xx00000x

(within error). We also used isothermal calorimetry (ITC) to determine CACs via a demicellisation experiment, diluting a concentrated SAMul ligand solution (Tris HCl 10 mM; NaCl 150 mM). Once again, all compounds exhibited similar CACs (Table 1). These values are slightly different to those determined by Nile Red assay, but that is to be expected as the experimental conditions are somewhat different (and in the case of ITC matched to the polyanion binding experiments, see below).

Table 1. Characterisation of C_{16}-L-Lys, C_{16}-D-Lys, C_{16}-Gly-L-Lys and C_{16}-Gly-D-Lys. Extracted CD data (λ_{max} and ellipticity), critical aggregation concentrations (CACs) from Nile Red (NR) assay (10 mM PBS, 45ºC) and ITC demicellisation experiments (10 mM Tris/HCl, 150 mM NaCl), DLS data (diameter and zeta potential, 10 mM Tris/HCl, 150 mM NaCl) .

	CD λ_{max} / nm [θ / mdeg]	NR CAC / μM	ITC CAC / μM	DLS Diameter / nm	DLS Zeta Pot / mV
C_{16}-L-Lys	218.5 [+5.1]	33 ± 3	45	6.2 ± 1.7	+45.2 ± 1.6
C_{16}-D-Lys	218.5 [-5.1]	29 ± 4	48	6.3 ± 1.7	+39.2 ± 1.6
C_{16}-Gly-L-Lys	230 [+1.3]	31 ± 3	49	120 ± 57	+40.1 ± 2.2
C_{16}-Gly-D-Lys	230 [-1.3]	28 ± 3	47	83 ± 50	+47.1 ± 1.4

Transmission electron microscopy (TEM) was used to visualise the self-assembled morphologies formed on drying aqueous solutions. All four compounds aggregated into similar micellar assemblies, with approximate diameters of ca. 8 nm (Fig. 3 and ESI). Dynamic light scattering (DLS) was used to further characterise these self-assembled nanostructures in solution (Table 1). Both C_{16}-L-Lys and C_{16}-D-Lys formed aggregates ca. 6.3 nm in diameter, assigned as spherical micelles. Perhaps surprisingly, however, C_{16}-Gly-L-Lys and C_{16}-Gly-D-Lys appeared to form larger solution-phase assemblies with diameters of ca. 120 nm and ca. 83 nm respectively, and large size distributions. Clearly C_{16}-Gly-L-Lys and C_{16}-Gly-D-Lys are more prone than C_{16}-L-Lys and C_{16}-D-Lys to further aggregation, which must stem from the molecular-level insertion of the glycine spacer. However, DLS was performed at elevated concentrations (0.5 mg ml^{-1}, 1 mM) which can impact on self-assembled morphology. We therefore also performed DLS at lower concentrations (down to 100 μM) to better reflect assay conditions, and found much greater contribution from smaller nanostructures (see ESI).

The zeta potentials of C_{16}-L-Lys, C_{16}-D-Lys, C_{16}-Gly-L-Lys and C_{16}-Gly-D-Lys were all similar and positive, reflecting protonation of lysine at physiological pH. As such, all systems formed self-assembled cationic nanostructures, expected to bind polyanionic heparin or DNA – the enantiomeric pairs existing as charge-dense identical (mirror-image) aggregates.

The DNA binding ability of C_{16}-L-Lys and C_{16}-D-Lys was initially quantified by displacement of ethidium bromide (EthBr) from its complex with DNA monitored by fluorescence spectroscopy in HEPES buffer (Fig. 2).[17] The CE_{50} value is the charge excess required for 50% displacement of EthBr, and EC_{50} is the concentration of binder at the same point (Table 2). The EC_{50} values are below the CACs of these ligands – it is well-known that polyanion binding can assist cationic lipid assembly by limiting electrostatic repulsion at the charged SAMul surface.[18] C_{16}-L-Lys and C_{16}-D-Lys had identical binding profiles (Fig. 2A) and identical CE_{50} values (Table 2), suggesting these enantiomeric self-assemblies bind DNA in identical ways – i.e., self-assembled nanoscale chirality has no significant impact on the molecular recognition interface. Conversely, the EthBr displacement assay indicated that the DNA binding ability of C_{16}-Gly-L-Lys and C_{16}-Gly-D-Lys was significantly different (Fig. 2C), with the former having a CE_{50} of 3.8 ± 0.7 but the latter having a CE_{50} of 1.5 ± 0.1, indicating much better binding (Table 2). Clearly DNA has a significant preference between these enantiomeric assemblies. This would suggest that on introducing the glycine spacer, the lysine ligands are better able to express their chirality at the nanoscale binding interface, and as such, the molecular structure of each ligand matters, rather than the overall charge density of the SAMul nanostructure being the only factor controlling binding.

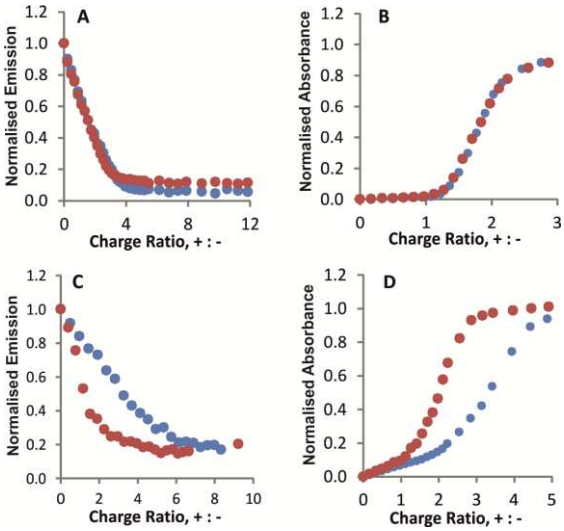

Figure 2. Graphs from competition assays. Top: C_{16}-L-Lys (blue) and C_{16}-D-Lys (red) with (A) DNA and (B) heparin. Bottom: C_{16}-Gly-L-Lys (blue) and C_{16}-Gly-D-Lys (red) with (C) DNA and (D) heparin. EthBr assays have [DNA] = 4 μM (per base) [EthBr] = 5.07 μM, in HEPES (2 mM), EDTA (0.05 mM) and NaCl (150 mM). MalB assays have [heparin] = 27 μM (per disaccharide) [MalB] = 25 μM, in Tris/HCl (10 mM) and NaCl (150 mM)

Table 2. DNA and heparin binding data for C_{16}-L-Lys, C_{16}-D-Lys, C_{16}-Gly-L-Lys and C_{16}-D-Lys extracted from competition assays with EthBr and MalB respectively. EthBr assays have [DNA] = 4 μM (per base) [EthBr] = 5.07 μM, in HEPES (2 mM), EDTA (0.05 mM) and NaCl (150 mM). MalB assays have [heparin] = 27 μM (per disaccharide) [MalB] = 25 μM, in Tris/HCl (10 mM) and NaCl (150 mM).

	DNA		Heparin	
	CE_{50}	EC_{50} / μM	CE_{50}	EC_{50} / μM
C_{16}-L-Lys	1.6 ± 0.2	3.2 ± 0.4	1.8 ± 0.1	100 ± 3
C_{16}-D-Lys	1.7 ± 0.1	3.4 ± 0.2	1.8 ± 0.1	100 ± 3
C_{16}-Gly-L-Lys	3.8 ± 0.7	7.6 ± 1.3	3.3 ± 0.3	180 ± 17
C_{16}-Gly-D-Lys	1.5 ± 0.1	3.1 ± 0.2	2.3 ± 0.1	122 ± 2

Heparin binding was quantified using a Mallard Blue (MalB) competition assay in which the displacement of MalB from its complex with heparin, is monitored by UV-vis spectroscopy.[19] The sigmoidal lineshape (Fig. 2) suggests that no binding takes place until the concentration of ligand exceeds a critical

concentration – as such, self-assembly is a pre-requisite for heparin binding. The CE_{50} values for C_{16}-L-Lys and C_{16}-D-Lys were identical (Table 2), indicating the chiral information at the nanoscale surface is not expressed in binding heparin. However, as for DNA binding, C_{16}-Gly-L-Lys and C_{16}-Gly-D-Lys had different perfomances (Fig. 2) with CE_{50} values of 1.7 ± 0.2 and 1.1 ± 0.1, respectively (Table 2). Chiral discrimination at the nanoscale binding interface has clearly, been switched on by the presence of the glycine spacer unit. As for DNA binding, C_{16}-Gly-D-Lys binds heparin significantly more effectively than enantiomeric C_{16}-Gly-L-Lys.

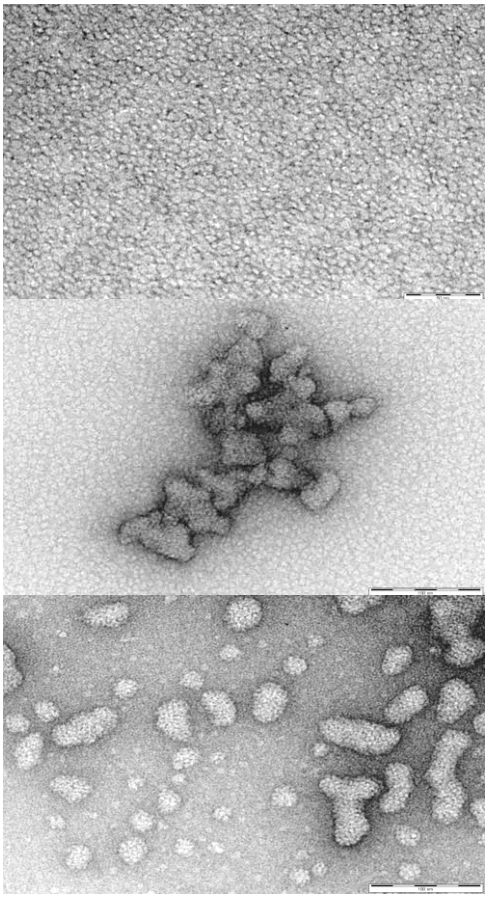

Figure 3. TEM images of self-assembled nanostructures formed by C_{16}-L-Lys. Images are taken in the absence of polyanion (top, scale bar = 50 nm); in the presence of heparin (middle, scale bar = 100 nm); in the presence of DNA (scale bar = 100 nm). All scale bars = 100 nm.

We were concerned that binding to polyanions may significantly disrupt the nanoscale self-assemblies, leading to structural reorganisation. We therefore used TEM to image the SAMul nanostructures in the presence of DNA and heparin. In all cases, and for both families of ligand, self-assembled micellar objects appeared to remain intact and co-assemble with the polyanionic components into clustered hierarchical structured nano-assemblies (Fig. 3 and ESI). This hierarchical assembly is a result of close packing between polycationic micellar spheres and polyanionic chains. The presence of 'un-bound' micelles in the TEM images arises from excess binder present in the samples. This imaging demonstrates that micellar stability is high and that self-assembly is not adversely affected by the presence of highly interactive polyanions.

Given the significant enantioselective binding differences induced by the introduction of a glycine spacer unit, we employed ITC titration methods to confirm these results and provide greater insight – detailed methodology is presented in the ESI – the SAMul systems were maintained well above their CAC throughout the titration in an attempt to avoid any thermodynamic contribution associated with de-micellisation. Binding isotherms are shown in Figure 4 and thermodynamic parameters are in Table 3. Overall, heparin is bound more strongly than DNA – primarily driven by the larger entropic term. In agreement with the EthBr/MalB displacement assays, the ITC results confirm that for C_{16}-L-Lys and C_{16}-D-Lys the self-assembled nanoscale chirality has no significant impact on the molecular recognition interface (Figs. 4A and B). Further, and once again in agreement with the competition assays, ITC indicated significant polyanion binding differences between C_{16}-Gly-L-Lys and C_{16}-Gly-D-Lys (Figs. 4C and D). Indeed, DNA displays a very clear preference for C_{16}-Gly-D-Lys over C_{16}-Gly-L-Lys, with ΔG_{bind} values of -28.1 kJ mol^{-1} and -25.5 kJ mol^{-1}, respectively ($\Delta\Delta G_{bind}$ = 2.6 kJ mol^{-1}). Furthermore, heparin binds somewhat better to C_{16}-Gly-D-Lys with ΔG_{bind} of -29.4 kJ mol^{-1} than the L enantiomer with ΔG_{bind} of -28.5 kJ mol^{-1} ($\Delta\Delta G_{bind}$ = 0.9 kJ mol^{-1}).

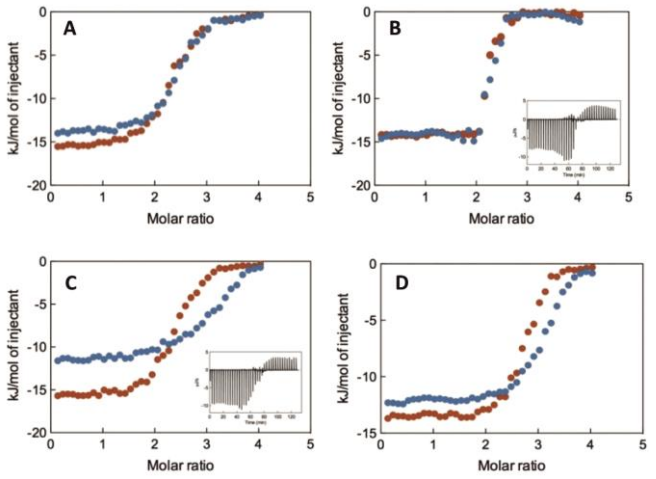

Figure 4. ITC traces. Top: C_{16}-L-Lys (blue) and C_{16}-D-Lys (red) with (A) DNA and (B) heparin (insert is measured heat power versus time elapsed during titration with C_{16}-D-Lys as an example). Bottom: C_{16}-Gly-L-Lys (blue) and C_{16}-Gly-D-Lys (red) with (A) DNA (insert is measured heat power versus time elapsed during titration with C_{16}-Gly-D-Lys as an example) and (B) heparin.

Polyanion binding in these SAMul systems is exothermic, as would be expected for ion-ion interactions. The ΔH_{bind} values for heparin binding are -13.7 and -12.3 kJ mol^{-1} for C_{16}-Gly-D-Lys and C_{16}-Gly-L-Lys respectively ($\Delta\Delta H_{bind}$ = 1.4 kJ mol^{-1})., and for DNA binding they are -15.7 and -11.6 kJ mol^{-1} respectively ($\Delta\Delta H_{bind}$ = 4.1 kJ mol^{-1}). The entropy values are positive, which suggests a degree of disorder induced by binding as solvent and ions are released from the nanoscale binding interface. Entropic differences between enantiomers are somewhat smaller. For heparin binding, $T\Delta S_{bind}$ values are +15.7 and +16.2 kJ mol^{-1} for the D- and L- systems respectively ($\Delta T\Delta S_{bind}$ = -0.5 kJ mol^{-1}), while for DNA binding, these values are +12.5 and +13.9 kJ mol^{-1} respectively ($\Delta T\Delta S_{bind}$ = -1.4 kJ mol^{-1}). As such, it is clear that the enhanced binding of C_{16}-Gly-D-Lys with DNA and also, to a lesser extent with heparin, is primarily of

enthalpic origin. This enhanced enthalpic effect is slightly offset by a smaller entropic gain for C_{16}-Gly-D-Lys, but enthalpy dominates. As such, we suggest that specific ligand-polyanion interactions are optimised on the surface of the C_{16}-Gly-D-Lys in comparison with C_{16}-Gly-L-Lys. The lower enantioselectivity of heparin towards these SAMul systems compared with DNA may result from the more polydisperse nature of heparin leading to a less well-defined distribution of anionic binding sites. In DNA, the structure of the polymer is more well-defined, with anionic sites evenly and repetitively spaced down the helical backbone, hence potentially benefitting more from an appropriately structured binding partner.

Table 3. DNA and heparin binding data for C_{16}-L-Lys, C_{16}-D-Lys, C_{16}-Gly-L-Lys and C_{16}-D-Lys extracted from ITC (10 mM Tris/HCl, 150 mM NaCl). All data are in $kJmol^{-1}$.

	DNA			Heparin		
	ΔG_{bind}	ΔH_{bind}	$-T\Delta S_{bind}$	ΔG_{bind}	ΔH_{bind}	$-T\Delta S_{bind}$
C_{16}-L-Lys	-27.3	-14.0	-13.3	-31.1	-14.6	-16.5
C_{16}-D-Lys	-27.7	-15.5	-12.1	-30.8	-14.2	-16.6
C_{16}-Gly-L-Lys	-25.5	-11.6	-13.9	-28.5	-12.3	-16.2
C_{16}-Gly-D-Lys	-28.1	-15.7	-12.5	-29.4	-13.7	-15.7

There are several potential reasons why the glycine spacer switches on enantioselective binding in this system. Most likely, as evidenced by DLS, is that the glycine spacer modifies the polarity and shape of the amphiphile and hence changes the self-assembled morphology, enabling the optimisation of the binding interface and greater selectivity. We can rule out any impact of charge density, as all systems have very similar zeta potentials. However, it is also possible that the additional glycine amide hydrogen bonding site may enable more specific interaction with the binding partner. Determining the relative importance of these different factors is the focus of a larger ongoing structure-activity relationship study. Clearly, however, polyanion binding is sensitive to the way ligands are displayed on the surface of SAMul nanostructures. Understanding such effects is important in predicting and understanding the selectivity of binding processes at self-assembled bio-surfaces, such as cell membranes, as well as in optimising binding to nanoscale biological targets such as these clinically important polyanions.

Notes and references

1 (*a*) M. Mammen, S. K. Choi and G. M. Whitesides, *Angew. Chem. Int. Ed.*, 1999, **37**, 2755-2794. (*b*) T. K. Dam and C. F. Brewer, *Glycobiology*, 2010, **20**, 270-279. (*c*) R. Nussinov and H. Jang, *Prog. Biophys. Mol. Biol.* 2014, **116**, 158-164.

2 (*a*) K. Riehemann, S. W. Schneider, T. A. Luger, B. Godin, M. Ferrari and H. Fuchs, *Angew. Chem. Int. Ed.*, 2009, **48**, 872-897. (*b*) D. A. Uhlenheuer, K. Petkau and L. Brunsveld, *Chem. Soc. Rev.*, 2010, **39**, 2817-2826. (*c*) E. Busseran, Y. Ruff, E. Moulin, N. Giuseppone, *Nanoscale* 2013, **5**, 7098-7140.

3 C. Fasting, C. A. Schalley, M. Weber, O. Seitz, S. Hecht, B. Koksch, J. Dernedde, C. Graf, E. W. Knapp and R. Haag, *Angew. Chem. Int. Ed.*, 2012, **51**, 10472-10498

4 (*a*) A. Barnard and D. K. Smith, *Angew. Chem. Int. Ed.*, 2012, **51**, 6572-6581. (*b*) K. Petkau-Milroy and L. Brunsveld, *Org. Biomol. Chem.*, 2013, **11**, 219-232.

5 (*a*) S. P. Jones, N. P. Gabrielson, D. W. Pack and D. K. Smith, *Chem. Commun.*, 2008, 4700-4702.(*b*) A. Barnard, P. Posocco, S. Pricl, M. Calderon, R. Haag, M. E. Hwang, V. W. T. Shum, D. W. Pack and D. K. Smith, *J. Am. Chem. Soc.*, 2011, **133**, 20288-20300. (*c*) A. Tschiche, A. M. Staedtler, S. Malhotra, H. Bauer, C. Böttcher, S. Sharbati, M. Calderon, M. Koch, T. M. Zollner, A. Barnard, D. K. Smith, R. Einspanier, N. Schmidt and R. Haag, *J. Mater. Chem. B*, 2014, **2**, 2153-2167.

6 (*a*) A. C. Rodrigo, A. Barnard, J. Cooper and D. K. Smith, *Angew. Chem. Int. Ed.*, 2011, **50**, 4675-4679. (*b*) S. M. Bromfield, P. Posocco, C. W. Chan, M. Calderon, S. E. Guimond, J. E. Turnbull, S. Pricl and D. K. Smith, *Chem. Sci.*, 2014, **5**, 1484-1492.

7 R. Srinivas, S. Samanta and A. Chaudhuri, *Chem. Soc. Rev.*, 2009, **38**, 3326-3338.

8 S. M. Bromfield, E. Wilde and D. K. Smith, *Chem. Soc. Rev.*, 2013, **42**, 9184-9185.

9 L. S. Jones, B. Yazzie and C.R. Middaugh, *Mol. Cell. Proteomics*, 2004, **3**, 746-769.

10 (*a*) D. Joester, M. Losson, R. Pugin, H. Heinzelmann, E. Walter, H. P. Merkle and F. Diederich, *Angew. Chem. Int. Ed.*, 2003, **42**, 1486-1490. (*b*) K. Rajangam, H. A. Behanna, M. J. Hui, X. Han, J. F. Hulvat, J. W. Lomasney and S. I. Stupp, *Nano Lett.*, 2006, **6**, 2086-2090. (*c*) S. K. M. Nalluri, J. Voskuhl, J. B. Bultema, E. J. Boekema and B. J. Ravoo, *Angew. Chem. Int. Ed.*, 2011, **50**, 9747-9751. (*d*) X. Liu, J. Zhou, T. Yu, C. Chen, Q. Cheng, K. Sengupta, Y. Huang, H. Li, C. Liu, Y. Wang, P. Posocco, M. Wang, Q. Cui, S. Giorgio, M. Fermeglia, F. Qu, S. Pricl, Y. Shi, Z. Liang, P. Rocchi, J. J. Rossi and L. Peng, *Angew. Chem. Int. Ed.*, 2014, **53**, 11822-11827. (*e*) G. L. Montalvo, Y. Zhang, T. M. Young, M. J. Costanzo, K. B. Freeman, J. Wang, D. J. Clements, E. Magavern, R. W. Kavash, R. W. Scott, D. H. Liu and W. F. DeGrado, *ACS Chem. Biol.*, 2014, **9**, 967-975.

11 (*a*) E. Kizilay, A. B. Kayitmazer and P. L. Dubin, *Adv. Colloid Interface Sci.* 2011, **167**, 24-37. (*b*) L. Chiappisi, I. Hoffmann and M. Gradzielski, *Soft Matter*, 2013, **9**, 3896-3909.

12 (*a*) A. Perico and A. Ciferri, *Chem. Eur. J.*, 2009, **15**, 6312-6320. (*b*) D. Li and N. J. Wagner, *J. Am. Chem. Soc.*, 2013, **135**, 17547-17555. (*c*) M. S. Sulatha and U. Natarajan, *J. Phys. Chem. B*, 2015, **119**, 12526-12539.

13 L. Fechner, B. Albanyan, V. M. P. Vieira, E. Laurini, P. Posocco, S. Pricl and D. K. Smith, *Chem. Sci.* 2016, **7**, 4653-4659.

14 S. M. Bromfield and D. K. Smith, *J. Am. Chem. Soc.*, 2015, **137**, 10056-10059.

15 J. Dey and A. Ghosh in *Chiral Separations by Capillary Eletrophoresis*, A. V. Eeckhaut and Y. Michotte (Eds.), CRC Press, Taylor and Francis, Boca Raton, 2009, pp 195-234.

16 M. C. A. Stuart, J. C. van de Pas and J. B. F. N. Engberts, *J. Phys. Org. Chem.* 2005, **18**, 929-934.

17 (*a*) B. F. Cain, B. C. Baguley and W. A. Denny, *J. Med. Chem.*, 1978, **21**, 658-668. (*b*) D. L. Boger, B. E. Fink, S. R. Brunette, W. C. Tse and M. P. Hedrick, *J. Am. Chem. Soc.*, 2001, **123**, 5878-5891.

18 (*a*) A. J. Konop and R. H. Colby, *Langmuir*, 1999, **15**, 58-65. (*b*) H. Schiessel, M. D. Correa-Rodriguez, S. Rudiuk, D. Baigl and K. Yoshikawa, *Soft Matter*, 2013, **8**, 9406-9411.

19 (*a*) S. M. Bromfield, A. Barnard, P. Posocco, M. Fermeglia, S. Pricl and D. K. Smith, *J. Am. Chem. Soc.*, 2013, **135**, 2911-2914. (*b*) S. M. Bromfield, P. Posocco, M. Fermeglia, S. Pricl, J. Rodríguez-López and D. K. Smith, *Chem. Commun.*, 2013, **49**, 4830-4832. (*c*) S. M. Bromfield, P. Posocco, M. Fermeglia, J. Tolosa, A. Herreros-López, J. Rodríguez-López and D. K. Smith, *Chem. Eur. J.* 2014, **20**, 9666-9674.

20 A. Mohanty and J. Dey, *J. Chrom. A*, 2006, **1128**, 259-266.

21 D. J. Welsh, P. Posocco, S. Pricl and D. K. Smith, *Org. Biomol. Chem.*, 2013, **11**, 3177-3186.

Journal Name

COMMUNICATION

Chiral recognition at self-assembled multivalent (SAMul) nanoscale surfaces – enantioselectivity in polyanion binding

Graphical Abstract

We investigate structure-activity effect relationships at the nanoscale chiral molecular recognition interface between enantiomeric self-assembled multivalent (SAMul) systems and biological polyanions, heparin and DNA.